Presented at Nonlinear Guided Wave Phenomena" Cambridge UK Sept 1991

558

Photonic Bloch Waves and Field Microstructure in Nonlinear Gratings: An Intuitive Approach

P.St.J. Russell,
Optoelectronics Research Centre,
University of Southampton,
Southampton SO9 5NH, U.K.

1. Introduction

Coupled wave theory is commonly used in numerical simulations of reflection from nonlinear grating structures. By contrast, the complementary photonic Bloch wave (PBW) approach has rarely been adopted, perhaps the only example being recent work on gap solitons[1,2]. Bloch wave theory[3,4] offers an alternative physical intuitive picture that encourages one to think in terms of field microstructure, leading to a range of simple explanations for the behaviour of light in linear gratings. In this paper the dispersion relation and field microstructure of *nonlinear* Bloch waves are found, and used to clarify the physical mechanisms that lead to regions of bistability, instability and oscillation for incidence of a monochromatic plane wave on a nonlinear grating half-space.

2. General nonlinear dispersion relation

The nonlinear Bloch waves are the grating's normal modes. In the two-wave approximation they are modelled by a pair of superimposed plane waves of constant amplitude:

$$E(z,t) = \frac{1}{2}\left(V_f \exp\{-j\mathbf{k}_f \cdot \mathbf{r}\} + V_b \exp\{-j\mathbf{k}_b \cdot \mathbf{r}\}\right) \exp(j\omega t) + \text{c.c.} \tag{1}$$

whose k-vectors are related by Floquet's theorem $\mathbf{k}_f = \mathbf{k}_b + \mathbf{K}$ where $|\mathbf{K}| = 2\pi/\Lambda$ is the grating vector and Λ its period. V_b and V_f are the field amplitudes and f and b are forward and backward labels. This pair of waves propagates through the grating with a fixed group velocity or decay rate. Putting (1) into Maxwell's equation, assuming a linear grating described by $\chi^{(1)} = \chi_o^{(1)} + \chi_m^{(1)} \cos(Kz)$, $\chi_m^{(1)} > 0$, and making standard approximations, it is straightforward to show that the field amplitudes obey:

$$\begin{pmatrix} -\delta_f + \Delta(|V_f|^2 + |V_b|^2) & \kappa + \Delta V_b^* V_f \\ \kappa + \Delta V_b V_f^* & \delta_b + \Delta(|V_f|^2 + |V_b|^2) \end{pmatrix} \begin{pmatrix} V_f \\ V_b \end{pmatrix} = \begin{pmatrix} 0 \\ 0 \end{pmatrix} \tag{2}$$

where $\kappa = \chi_m^{(1)} k_o / 4n_o^2$, and the nonlinear dephasing parameter Δ is

$$\Delta = \left[3\chi^{(3)}\omega\mu S_o / 8(1 + \chi_o^{(1)})\right). \tag{3}$$

where S_o is the incident Poynting vector. δ_f and δ_b are the corrections to the mean linear wavevector k_o needed to yield $\mathbf{k}_f$ and $\mathbf{k}_b$, i.e.,

$$\mathbf{k}_n^2 \;=\; (k_o + \delta_n)^2.$$

Solutions of (2) are easily found algebraically for a given boundary condition, yielding up to three different (δ_f, δ_b, V_f/V_b) sets and hence three different nonlinear Bloch waves.

For a purely distributed feed-back (DFB) structure (Figure 1), $\mathbf{k}_b$ and $\mathbf{k}_f$ are anti-parallel, and we write

$$\gamma = \delta_f = (\delta_b - \vartheta) \tag{4}$$

Figure 1: Boundary condition at DFB half-space.

where $\vartheta = 2k_o - K = 2n_o(\omega - \omega_B)/c \approx 4\pi n_o(\lambda_B - \lambda)/\lambda_B^2$ and λ_B is the vacuum Bragg wavelength. The parameter γ is the perturbation to k_o that appears in the vicinity of a Bragg condition, i.e., $k_f = k_o + \gamma$.

As written, the matrix equation (2) illustrates succinctly the various regions of behaviour. At $\Delta = 0$, the standard linear dispersion relation is obtained, as illustrated in Figure 1 for Bloch waves with group velocities pointing into the grating. Floquet's theorem forces the field microstructure (created by interference) to mimic the grating structure. Fast and slow PBW's exist, for which the optical power is partially or fully redistributed by interference into, respectively, the low and high refractive index regions of the grating. For linear gratings, the ramifications of this picture are fully explored in a separate article[4].

As the nonlinearity rises, the mean wavevectors in the grating are increased by $\Delta(|V_f|^2 + |V_b|^2)$ (on-diagonal matrix elements) and the effective grating strength by $\Delta V_b V_f^*$ (off-diagonal matrix elements). The fringe microstructure of the Bloch wave, having the same periodicity as the grating, acts either to enhance or reduce the grating strength. A fast PBW in a grating with a positive Δ will experience a gradual diminution in grating strength, leading to modulational instability when the induced nonlinear grating cancels the linear one at

$$\kappa = -\Delta V_b^* V_f. \tag{5}$$

The slow PBW's, on the other hand, will experience a nonlinear enhancement in grating strength as the power is raised. Concurrently with these effects, the average refractive index of the material rises. The full picture is thus of a complex interplay of Bragg condition dephasing and grating enhancement/depletion.

3. Dispersion diagrams

This behaviour may be summarised graphically on a k_f–ϑ diagram, as depicted on Figure 2 for the special case of plane-wave incidence on a DFB half-space (Figure 1). Under these circumstances the boundary condition at $z = 0$ is very simple: $V_f = 1$ (the normalised amplitude of the incident plane wave) and $V_b = \pm\sqrt{\eta}$ where $0 \leq \eta \leq 1$ is the reflection efficiency. For each value of ϑ, the matrix equation is then solved for permitted values of γ and V_b and the results plotted on the k_f–ϑ diagram. A succession of different cases is now explored: (a) In the absence of a grating, the solution is the straight line $(\gamma + \theta)/\kappa = -\Delta/\kappa - \vartheta/2\kappa$ expected of a monochromatic plane wave travelling into the grating half-space. It is the sloping (-..-..) line on the diagrams. (b) Introducing a linear grating, the usual stop-band opens up at the Bragg condition. The branches with negative group velocities ($\partial k_f/\partial\vartheta < 0$) are suppressed – they play no role in the grating half-space. On its red-shifted branch, the k–vector is longer than predicted in (a), i.e., the PBW is a slow one. The opposite is true on the blue-shifted branch. As mentioned above, this behaviour is the result of the periodic PBW field microstructure; power is redistributed into low/high index regions. (c) Increasing the optical nonlinearity or the input power level, two effects are seen: i) as expected from very simple considerations, the Bragg condition shifts to lower frequencies owing to the nonlinear increase in the average propagation constant; ii) the stop-band branches gradually develop distortions owing to the appearance

of a nonlinear grating through interference of the backward and forward waves in the Bloch wave. These distortions are most severe where the nonlinear grating is strongest, i.e., close to the band edges where the fringe visibility is greatest.

4. Refractive index profiles

The linear, nonlinear and nett refractive index profiles across the grating planes are plotted in Figure 2 for ten different Bloch waves. In cases 1 and 3, the nett grating strength is zero, meaning that the forward and backward waves are no longer bound together – this will cause modulational instability. In cases 1,3 and 5 the nonlinear grating strength actually *exceeds* the linear, reversing the sign of its grating ripple: a fast Bloch wave turns into a slow. In all these cases the Bloch waves are likely to be unstable since the nonlinear grating equals or dominates over the linear.

On the slow stop-band side at intermediate levels of nonlinearity, parameter regimes exist where the nonlinear PBW is "evanescent", whereas the linear PBW is propagating. This occurs at $\vartheta/2\kappa = -2.5$ for $\Delta/\kappa = 1$ in Figure 2. The analysis here is not valid in these regions, since evanescence is not compatible with stability for nonlinear waves, for the level of optical nonlinearity will fall off as the PBW amplitude decays; at some point inside the DFB structure the PBW will start to propagate, causing light to leak through and violating the evanescent condition. It is likely that instability and oscillation will occur in this range.

For high levels of nonlinearity, the stop-band ceases to exist, although the region of modulational instability (approximately between points 3 and 5) widens. On the red-shifted stop-band branch, however, bistability arises where two or more travelling-wave solutions exist, with high and low reflection states.

5. General discussion and conclusions

To observe the effects described here, the nonlinear index change must be comparable to the index modulation depth of the linear grating. The two waves bound together by the grating forms an entity insensitive against weak perturbations. Slight changes in refractive index ($\Delta/\kappa \ll 1$) will slow down or speed up the Bloch wave without disturbing its field microstructure or group velocity dispersion. This occurs for example on the edge of the blue-shifted stop-band, where the negative GVD of the linear Bloch waves is undisturbed by the nonlinear index changes needed for gap soliton formation. A quite different situation occurs when $\Delta/\kappa \sim 1$, for now the nonlinear index perturbation is comparable to the grating index modulation and the Bloch wave entity is susceptible to gross distortions in its normal mode shape. This is reflected in the stop-band distortions seen in Figure 2. An interesting aspect of this regime is that the optical path length does not determine whether strong nonlinear effects are seen or not; they are caused by modal shape distortions and not cumulative phase delays between co-propagating waves.

For a grating of modulation depth 10^{-5} at $\lambda_B = 1\mu$m in an optical fibre with $n_2 \approx 3 \times 10^{-8}$ μm^2/Watt and a core area of 1 μm^2, a power level of a few 100 Watts would result in the behaviour depicted in Figure 2. In order not to straddle the whole stop-band at once, the incident bandwidth would need to be of the order of 10^{-6} of the optical base frequency, i.e., some 0.3 GHz.

In conclusion, the nonlinear PBW approach leads to an easily solvable algebraic dispersion relation, a clear field-microstructural explanation for PBW behaviour, and may be used to delineate regions of stability and instability for incidence on a grating half-space.

References

1. J.E. Sipe and H.G. Winful, Optics Letters **13** (133-134) 1988.
2. C.M. de Sterke and J.E. Sipe, Phys.Rev.Lett. **63**(811) 1989.
3. P.St.J. Russell, Phys.Rev. A **33** (3232-3242) 1986.
4. P.St.J. Russell, J.Mod.Optics, in press.

Figure 2: Stop-bands and refractive index profiles for several different cases. The slanting (-..-..) lines on the stop-band diagrams are the solutions for a plane wave in an isotropic nonlinear medium. The loci of forward travelling Bloch waves alone are included (the backward travelling waves do not appear in a half-space). The refractive index profiles show the original grating (-.-.), the nonlinear index change (-..-..) and the nett index profile (—). Cancellation of the linear grating occurs at points 1 and 3, where modulational instability is expected. All the nonlinear distortions in the stop-band shape can be understood from these index modulation patterns. The branches (terminating at 4 and 5, and 1 and 2) are algebraically asymptotic to the dashed lines $(\gamma + \vartheta/2) = -\Delta - \vartheta/6$.

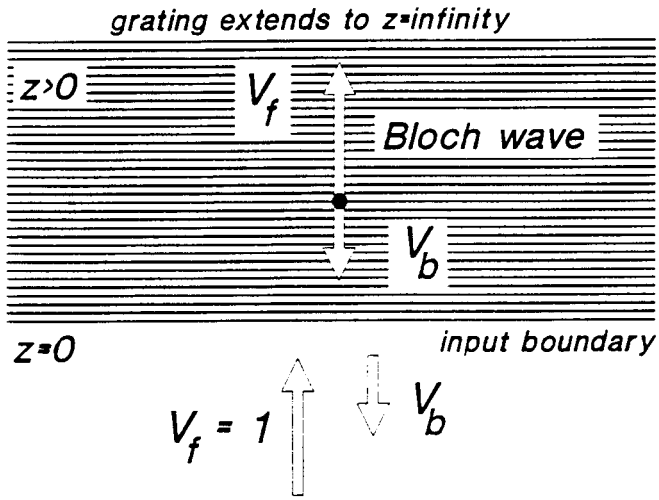
grating extends to z=infinity
z>0
V_f
Bloch wave
V_b
z=0
input boundary
$V_f = 1$
V_b

Fig 1

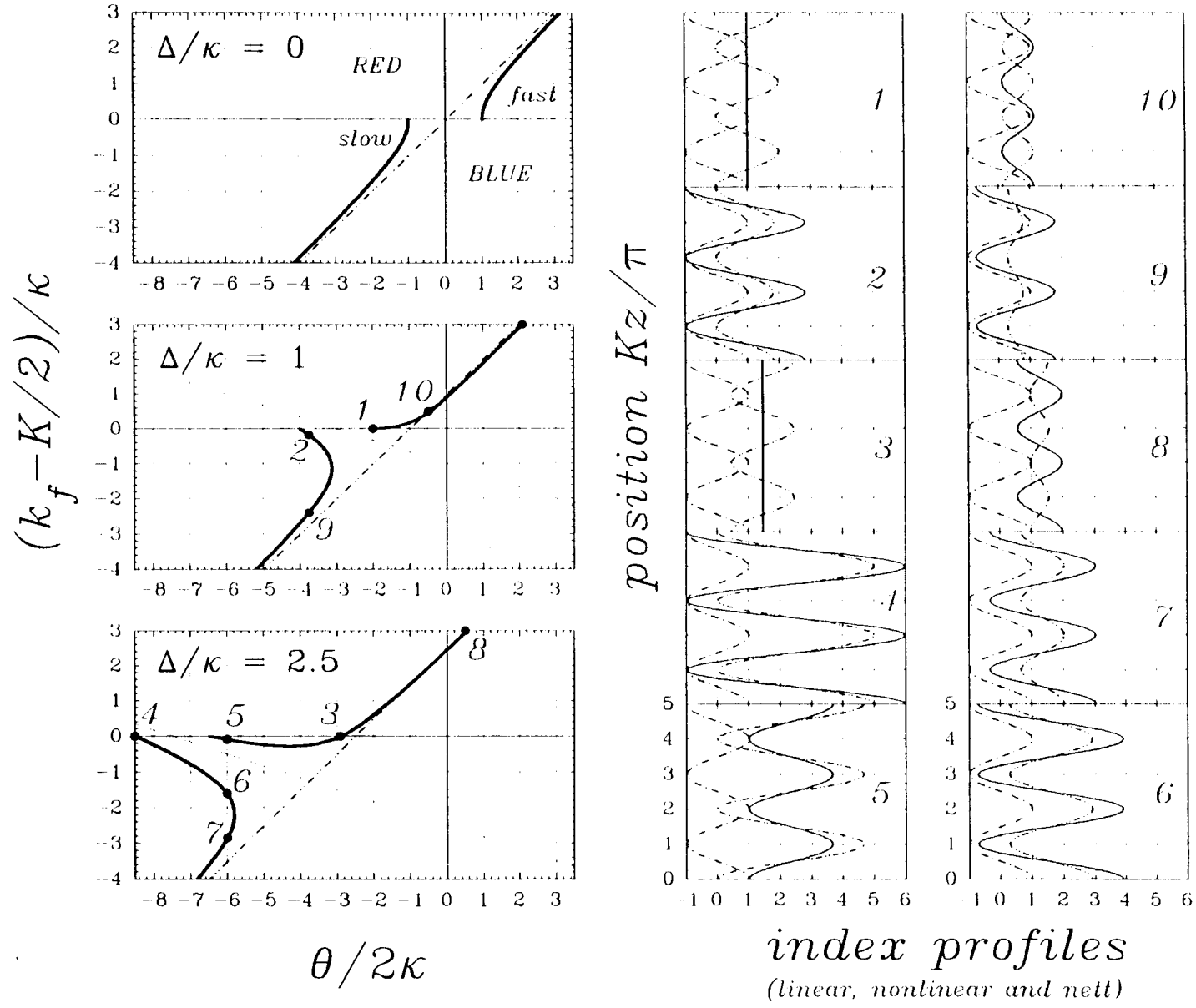
Δ/κ = 0
RED
fast
slow
BLUE
Δ/κ = 1
1
10
2
9
Δ/κ = 2.5
8
4
5
3
6
7
(k_f − K/2)/κ
θ/2κ
position Kz/π
1
10
2
9
3
8
4
7
5
6
index profiles
(linear, nonlinear and nett)